



A screw dislocation near a coated non-elliptical inhomogeneity with internal uniform stresses

Xu Wang^{a,*}, Liang Chen^a, Peter Schiavone^{b,*}

^a School of Mechanical and Power Engineering, East China University of Science and Technology, 130 Meilong Road, Shanghai 200237, China

^b Department of Mechanical Engineering, University of Alberta, 10-203 Donadeo Innovation Centre for Engineering, Edmonton, Alberta T6G 1H9, Canada



ARTICLE INFO

Article history:

Received 21 September 2018

Accepted 14 December 2018

Available online 22 January 2019

Keywords:

Conformal mapping

Complex variable method

Anti-plane elasticity

Coating

Non-elliptical inhomogeneity

Internal uniform stress field

ABSTRACT

We consider the anti-plane shear deformation of a three-phase inhomogeneity-coating-matrix composite containing a coated non-elliptical inhomogeneity whose surrounding matrix is subjected to the action of a screw dislocation and uniform remote anti-plane shear stresses. Our objective is to establish conditions under which the inhomogeneity maintains an internal uniform stress field. Our analysis, which is based on a carefully chosen conformal mapping function, clearly indicates that such an internal uniform stress distribution can be achieved independently of the action of the screw dislocation, which influences the shape of the inhomogeneity depending on its proximity to the dislocation. In fact, we find that when the screw dislocation is located far from the coated inhomogeneity, the corresponding material interfaces become two confocal ellipses as reported previously in the literature. A simple criterion for the convergence of the series in the conformal mapping function is established.

© 2018 Académie des sciences. Published by Elsevier Masson SAS. All rights reserved.

1. Introduction

In the design of fiber-reinforced composites, it is commonplace to introduce an intermediate layer consisting of a thin or thick coating between the internal fiber (or the inhomogeneity) and the surrounding matrix to improve the overall mechanical performance of the composite (see, for example, [1–5]). For example, the coating is often used to improve the quality of fiber–matrix bonding as well as to reduce stress concentrations at the fiber–matrix interface. Uniformity of an internal stress distribution has been observed in the following cases when the composite is subjected to uniform remote anti-plane shearing: in a three-phase concentric circular inhomogeneity; a three-phase confocal elliptical inhomogeneity; and in a three-phase non-elliptical inhomogeneity with appropriately designed coating thickness (see, respectively, Ru and Schiavone [6], Ru et al. [7], Wang and Gao [8]). It has also been observed that the stress field within a three-phase concentric circular inhomogeneity interacting with a screw dislocation is intrinsically non-uniform [9]. However, it has been shown quite recently that the internal stress distribution can indeed remain uniform within a single or even two non-elliptical inhomogeneities interacting with a screw dislocation when the inhomogeneities are assumed to be perfectly bonded to the surrounding matrix (i.e. in the absence of any coating) [10,11].

* Corresponding authors.

E-mail addresses: xuwang@ecust.edu.cn (X. Wang), p.schiavone@ualberta.ca (P. Schiavone).

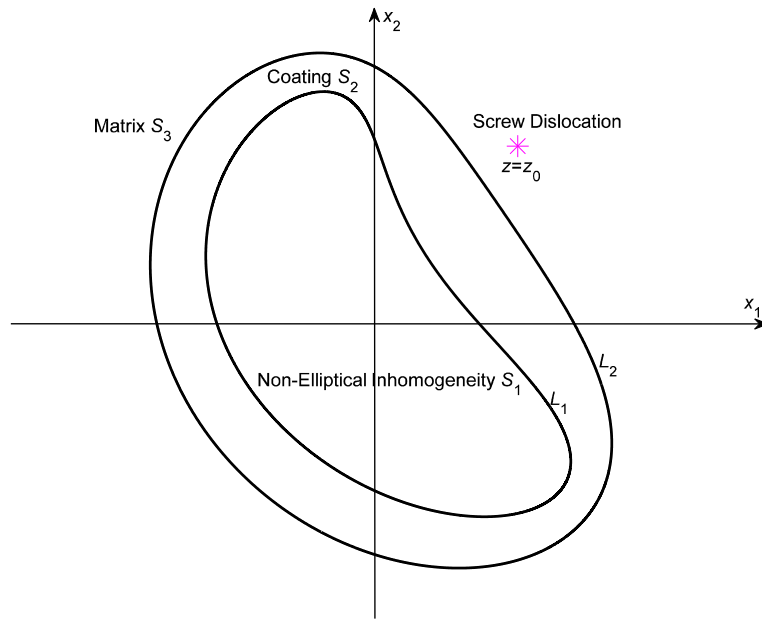


Fig. 1. A coated non-elliptical inhomogeneity interacting with a screw dislocation.

Recognizing that an internal uniform stress distribution is optimal in the sense that it eliminates stress peaks within the inhomogeneity, we continue our investigations by establishing conditions under which a non-elliptical inhomogeneity surrounded by a coating of separate elastic properties can be designed to maintain the desired uniform internal stress distribution when the corresponding composite is subjected to anti-plane shear deformations with prescribed uniform remote stresses and the action of a screw dislocation somewhere in the matrix. Interestingly, the internal uniform stress field inside the inhomogeneity is found to be independent of the action of the screw dislocation whilst the shape of the coated inhomogeneity is influenced by the presence of a nearby screw dislocation. The two non-elliptical interfaces of the three-phase composite as well as the location of the screw dislocation, which permit the desired internal uniform stress field, can be conveniently designed via the introduction of a particular conformal mapping function which maps the region occupied by the coating and the matrix onto the exterior of the unit circle in the image ξ -plane. A simple criterion for the convergence of the series in the conformal mapping function is established based on the D'Alembert's ratio test.

2. Formulation

Under anti-plane shear deformations of an isotropic elastic material, the two shear stress components σ_{31} and σ_{32} , the out-of-plane displacement w and the stress function ϕ can be expressed in terms of a single analytic function $f(z)$ of the complex variable $z = x_1 + ix_2$ as [12]

$$\sigma_{32} + i\sigma_{31} = \mu f'(z), \quad \phi + i\mu w = \mu f(z) \tag{1}$$

where μ is the shear modulus, and the two stress components can be expressed in terms of the single stress function as [12]

$$\sigma_{32} = \phi_{,1}, \quad \sigma_{31} = -\phi_{,2} \tag{2}$$

Let S_1, S_2 and S_3 denote the internal inhomogeneity, the intermediate coating and the surrounding unbounded matrix, respectively, all of which are perfectly bonded through the inner and outer non-elliptical interfaces L_1 and L_2 , as shown in Fig. 1. The matrix is subjected to uniform anti-plane shear stresses at infinity ($\sigma_{31}^\infty, \sigma_{32}^\infty$) and the action of a screw dislocation with Burgers vector b applied at $z = z_0$ (see Fig. 1). Our main objective is to examine whether uniform stresses remain possible inside the internal (non-elliptical) inhomogeneity even in the presence of the nearby screw dislocation. In what follows, the subscripts 1, 2 and 3 are used to identify the respective quantities in S_1, S_2 and S_3 .

3. Internal uniform stress field

The boundary value problem for the three-phase composite takes the following form

$$\begin{aligned} f_2(z) + \overline{f_2(z)} &= \Gamma_1 f_1(z) + \Gamma_1 \overline{f_1(z)} \\ f_2(z) - \overline{f_2(z)} &= f_1(z) - \overline{f_1(z)}, \quad z \in L_1 \end{aligned} \tag{3a}$$

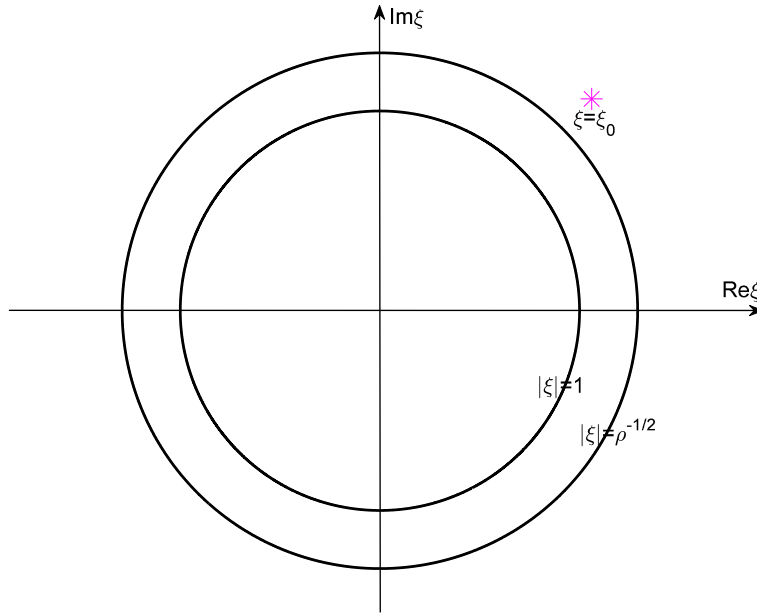


Fig. 2. The problem in the ξ -plane.

$$f_3(z) + \overline{f_3(z)} = \Gamma_2 f_2(z) + \Gamma_2 \overline{f_2(z)} \tag{3b}$$

$$f_3(z) - \overline{f_3(z)} = f_2(z) - \overline{f_2(z)}, \quad z \in L_2$$

$$f_3(z) \cong \frac{b}{2\pi} \ln(z - z_0) + O(1), \quad z \rightarrow z_0 \tag{3c}$$

$$f_3(z) \cong \frac{\sigma_{32}^\infty + i\sigma_{31}^\infty}{\mu_3} z + \frac{b}{2\pi} \ln z + O(1), \quad |z| \rightarrow \infty \tag{3d}$$

where Γ_1 and Γ_2 are two stiffness ratios defined by

$$\Gamma_1 = \frac{\mu_1}{\mu_2}, \quad \Gamma_2 = \frac{\mu_2}{\mu_3} \tag{4}$$

Equations (3a) and (3b) describe the continuity conditions of traction and displacement across the inner and outer perfect interfaces L_1 and L_2 , respectively; Eq. (3c) characterizes the singular behavior of $f_3(z)$ at the location of the screw dislocation $z = z_0$; Eq. (3d) gives the remote asymptotic behavior of $f_3(z)$ due to the remote loading and the Burgers vector of the screw dislocation.

To solve the above boundary value problem, it is more convenient to introduce the following conformal mapping function

$$z = \omega(\xi), \quad \xi = \omega^{-1}(z), \quad |\xi| \geq 1 \tag{5}$$

the specific form of which is to be determined in the ensuing analysis. Using this mapping function, the exterior of the inhomogeneity (a simply-connected domain) is mapped onto the exterior of the unit circle in the ξ -plane. More specifically, as shown in Fig. 2, the regions S_2 and S_3 are mapped onto $1 \leq |\xi| \leq \rho^{-\frac{1}{2}}$ and $|\xi| \geq \rho^{-\frac{1}{2}}$, respectively; the two interfaces L_1 and L_2 are mapped onto the two concentric circles $|\xi| = 1$ and $|\xi| = \rho^{-\frac{1}{2}}$; the location of the screw dislocation $z = z_0$ is mapped onto $\xi = \xi_0$ (i.e., $z_0 = \omega(\xi_0)$ or $\xi_0 = \omega^{-1}(z_0)$). Here ρ ($0 < \rho < 1$) can be considered as a dimensionless parameter measuring the relative thickness of the coating. In order to ensure that the mapping in Eq. (5) is “one-to-one” for $z \in S_2 \cup S_3$, it is necessary that $\omega'(\xi) \neq 0$ for $|\xi| > 1$. For convenience and without loss of generality, we write $f_2(\xi) = f_2(\omega(\xi))$ and $f_3(\xi) = f_3(\omega(\xi))$.

To ensure that the internal stresses inside the inhomogeneity are uniform, $f_1(z)$ defined in the inhomogeneity must take the following form:

$$f_1(z) = kz, \quad z \in S_1 \tag{6}$$

where k is a complex number to be determined.

By enforcing continuity of traction and displacement across the inner interface L_1 in Eq. (3a), we arrive at the following expression for $f_2(\xi)$

$$f_2(\xi) = \frac{k(\Gamma_1 + 1)}{2}\omega(\xi) + \frac{\bar{k}(\Gamma_1 - 1)}{2}\bar{\omega}\left(\frac{1}{\xi}\right), \quad 1 \leq |\xi| \leq \rho^{-\frac{1}{2}} \tag{7}$$

Similar conditions across the outer interface L_2 in Eq. (3b) lead to the following expression for $f_3(\xi)$

$$f_3(\xi) = \frac{k(\Gamma_1 + 1)(\Gamma_2 + 1)}{4}\omega(\xi) + \frac{k(\Gamma_1 - 1)(\Gamma_2 - 1)}{4}\omega(\rho\xi) + \frac{\bar{k}(\Gamma_1 - 1)(\Gamma_2 + 1)}{4}\bar{\omega}\left(\frac{1}{\xi}\right) + \frac{\bar{k}(\Gamma_1 + 1)(\Gamma_2 - 1)}{4}\bar{\omega}\left(\frac{1}{\rho\xi}\right), \quad |\xi| \geq \rho^{-\frac{1}{2}} \tag{8}$$

A careful inspection of the above expression suggests that it is sufficient for our purposes to adopt the mapping function in the following specialized form

$$z = \omega(\xi) = R\left(\xi + \frac{p}{\xi} + \sum_{j=1}^{+\infty} q_j \ln \frac{\xi - \rho^{j-1}\bar{\xi}_0^{-1}}{\xi}\right), \quad |\xi| \geq 1 \tag{9}$$

where R is a real scaling constant, p is a given complex constant, $q_j, j = 1, 2, \dots, +\infty$ are complex constants to be determined. The branch cut for the multi-valued logarithmic function $\ln \frac{\xi - \rho^{j-1}\bar{\xi}_0^{-1}}{\xi}$ in Eq. (9) is chosen to be the line segment within the unit circle connecting $\xi = \rho^{j-1}\bar{\xi}_0^{-1}$ and $\xi = 0$. Thus, all the logarithmic functions appearing in Eq. (9) for different values of j are analytic and single-valued for $|\xi| \geq 1$. Note that by using the mapping function in Eq. (9), $f_2(\xi)$ given by Eq. (7) is analytic and single-valued in its region of definition $1 \leq |\xi| \leq \rho^{-\frac{1}{2}}$ since each of the logarithmic functions $\ln(\xi - \rho^{1-j}\bar{\xi}_0)$, $j = 1, 2, \dots, +\infty$ appearing in $\bar{\omega}\left(\frac{1}{\xi}\right)$ are analytic and single-valued in $1 \leq |\xi| \leq \rho^{-\frac{1}{2}}$ in view of the fact that $\rho^{1-j}|\bar{\xi}_0| > \rho^{-\frac{1}{2}}, j = 1, 2, \dots, +\infty$.

By substituting Eq. (9) into Eq. (8) and ensuring that $f_3(\xi)$ is regular at the points $\xi = \rho^{-j}\bar{\xi}_0, j = 1, 2, \dots, +\infty$ and that it exhibits the logarithmic singularity at $\xi = \bar{\xi}_0$ in Eq. (3c), we obtain the following recurrence relation

$$q_{j+1} = \Lambda q_j, \quad j = 1, 2, \dots, +\infty \tag{10}$$

where Λ is a real material parameter defined by

$$\Lambda = \frac{(\Gamma_1 + 1)(1 - \Gamma_2)}{(\Gamma_1 - 1)(\Gamma_2 + 1)} \tag{11}$$

and

$$q_1 = q = \frac{2b}{\pi k R (\Gamma_1 - 1)(\Gamma_2 + 1)} \tag{12}$$

Using Eqs. (10) and (12), the mapping function in Eq. (9) can now be further specified as

$$z = \omega(\xi) = R\left(\xi + \frac{p}{\xi} + q \sum_{j=0}^{+\infty} \Lambda^j \ln \frac{\xi - \rho^j \bar{\xi}_0^{-1}}{\xi}\right), \quad |\xi| \geq 1 \tag{13}$$

which indicates that the non-elliptical shape of the coated inhomogeneity and the location of the screw dislocation can be readily determined once the five parameters p, q, ρ, Λ and $\bar{\xi}_0$ are known. As $|\bar{\xi}_0| \rightarrow \infty$ (i.e., the screw dislocation is located far from the coated inhomogeneity), the interfaces become two confocal ellipses as observed by Ru et al. [7] in the absence of the screw dislocation.

By using D'Alembert's ratio test, it is seen that the series in the mapping function (13) is convergent when $\rho|\Lambda| < 1$. The specific procedure is as follows: if we set $b_j = \Lambda^j \ln \frac{\xi - \rho^j \bar{\xi}_0^{-1}}{\xi}$ in Eq. (13), then

$$\lim_{j \rightarrow \infty} \left| \frac{b_{j+1}}{b_j} \right| = |\Lambda| \lim_{j \rightarrow \infty} \left| \frac{\ln(1 - \rho^{j+1}\bar{\xi}_0^{-1}\xi^{-1})}{\ln(1 - \rho^j\bar{\xi}_0^{-1}\xi^{-1})} \right| = |\Lambda| \lim_{j \rightarrow \infty} \left| \frac{\sum_{n=1}^{\infty} \frac{(\rho^{j+1}\bar{\xi}_0^{-1}\xi^{-1})^n}{n}}{\sum_{n=1}^{\infty} \frac{(\rho^j\bar{\xi}_0^{-1}\xi^{-1})^n}{n}} \right| = \rho|\Lambda|$$

from which the convergence criterion is established. It is clear that the series in Eq. (13) is also analytic, single-valued and convergent for the annulus $\rho^{\frac{1}{2}} \leq |\xi| \leq 1$ in addition to the region $|\xi| \geq 1$ by considering the fact that all the logarithmic singularities in Eq. (13) are located within the circle $|\xi| = \rho^{\frac{1}{2}}$.

Remark. Using Eq. (13), the sum of the two terms containing analytic continuations in Eq. (8) will finally become as follows after appropriate cancellations:

$$\begin{aligned} & \frac{\bar{k}(\Gamma_1 - 1)(\Gamma_2 + 1)}{4} \bar{\omega}\left(\frac{1}{\xi}\right) + \frac{\bar{k}(\Gamma_1 + 1)(\Gamma_2 - 1)}{4} \bar{\omega}\left(\frac{1}{\rho\xi}\right) \\ &= \frac{\bar{k}\bar{q}R(\Gamma_1 - 1)(\Gamma_2 + 1)}{4} \ln(\xi - \xi_0) + \frac{R\bar{k}(\Gamma_1 - 1)(\Gamma_2 + 1)}{4} \left(\frac{1}{\xi} + \bar{p}\xi\right) + \frac{R\bar{k}(\Gamma_1 + 1)(\Gamma_2 - 1)}{4} \left(\frac{1}{\rho\xi} + \bar{p}\rho\xi\right) \end{aligned}$$

whilst both $\omega(\xi)$ and $\omega(\rho\xi)$ in Eq. (8) are analytic for $|\xi| \geq \rho^{-\frac{1}{2}}$ except at infinity by considering the fact that $\omega(\xi)$ is analytic in $|\xi| \geq \rho^{\frac{1}{2}}$ again except at infinity.

By enforcing the remote asymptotic condition in Eq. (3d), we arrive at the following relationship

$$k[(\Gamma_1 + 1)(\Gamma_2 + 1) + \rho(\Gamma_1 - 1)(\Gamma_2 - 1)] + \bar{p}\bar{k}[(\Gamma_1 - 1)(\Gamma_2 + 1) + \rho(\Gamma_1 + 1)(\Gamma_2 - 1)] = \frac{4(\sigma_{32}^\infty + i\sigma_{31}^\infty)}{\mu_3} \tag{14}$$

through which the complex number k can be uniquely determined as

$$k = \frac{4(\sigma_{32}^\infty + i\sigma_{31}^\infty)[(\Gamma_1 + 1)(\Gamma_2 + 1) + \rho(\Gamma_1 - 1)(\Gamma_2 - 1)] - 4\bar{p}(\sigma_{32}^\infty - i\sigma_{31}^\infty)[(\Gamma_1 - 1)(\Gamma_2 + 1) + \rho(\Gamma_1 + 1)(\Gamma_2 - 1)]}{\mu_3\{[(\Gamma_1 + 1)(\Gamma_2 + 1) + \rho(\Gamma_1 - 1)(\Gamma_2 - 1)]^2 - |\rho|^2[(\Gamma_1 - 1)(\Gamma_2 + 1) + \rho(\Gamma_1 + 1)(\Gamma_2 - 1)]^2\}} \tag{15}$$

It follows from Eqs. (1) and (6) that the internal stresses are uniformly distributed inside the inhomogeneity according to

$$\sigma_{32} + i\sigma_{31} = \mu_1 k, \quad z \in S_1 \tag{16}$$

It is then clearly seen from Eqs. (15) and (16) that the internal uniform stress field inside the inhomogeneity is independent of the action of the screw dislocation. By using Eq. (15), the complex parameter q in Eq. (12) can then be uniquely expressed in terms of the remote loading $(\sigma_{31}^\infty, \sigma_{32}^\infty)$, the Burgers vector b , the two stiffness ratios Γ_1 and Γ_2 , the shear modulus μ_3 of the matrix, the given complex number p and the scaling constant R . It is seen that when q is a real number, $\sigma_{31}^\infty = 0$ and $\sigma_{32}^\infty \neq 0$, whereas when q is a purely imaginary number we have $\sigma_{32}^\infty = 0$ and $\sigma_{31}^\infty \neq 0$. Apparently, the non-elliptical shape of the coated inhomogeneity derives solely from the existence of the screw dislocation in the matrix.

4. Numerical examples

For our calculations, the series in Eq. (13) is truncated at $j = 100$. In this section, several specific numerical examples will be presented to demonstrate the analytical results obtained in the previous section. In fact, Fig. 1 is obtained by adopting the following parameters:

$$p = 0.2, \quad q = 0.5, \quad \rho = 0.6, \quad \Lambda = 0.4, \quad \xi_0 = 1.5 \exp\left(\frac{i\pi}{4}\right) \tag{17}$$

In what follows, the shape of the coated inhomogeneity and the location of the screw dislocation are shown in Figs. 3–5 for the following respective sets of parameters:

$$p = 0.2, \quad q = 0.5, \quad \rho = 0.8, \quad \Lambda = 0.4, \quad \xi_0 = 1.5 \tag{18}$$

$$p = 0, \quad q = 0.5i, \quad \rho = 0.8, \quad \Lambda = 0.4, \quad \xi_0 = 1.5 \tag{19}$$

$$p = 0, \quad q = -0.5, \quad \rho = 0.8, \quad \Lambda = -0.4, \quad \xi_0 = 1.5 \tag{20}$$

As a fifth example, the shape of the coated inhomogeneity and the location of the screw dislocation are shown in Fig. 6 when

$$p = 0.2, \quad q = 0.334, \quad \rho = 0.8, \quad \Lambda = 1, \quad \xi_0 = 1.5 \tag{21}$$

Here $\Lambda = 1$ implies that the inhomogeneity and the matrix have the same shear modulus (i.e., $\mu_1 = \mu_3$). We see from Fig. 6 that one part of the inner interface almost touches another part.

As a sixth example, we consider the case when (see Fig. 7)

$$p = 0, \quad q = -0.5, \quad \rho = 0.8, \quad \Lambda = -1, \quad \xi_0 = 1.343 \tag{22}$$

Here $\Lambda = -1$ implies that $\mu_2 = \sqrt{\mu_1\mu_3}$. From Fig. 7, we can see the presence of a sharp corner on the inner interface.

In the next example (Fig. 8) we consider a case when $\Lambda > 1$:

$$p = 0.2, \quad q = 0.5, \quad \rho = 0.5, \quad \Lambda = 1.2, \quad \xi_0 = 2 \tag{23}$$

Here, despite the fact that $\Lambda > 1$, the series in Eq. (13) remains convergent in view of the fact that $\rho|\Lambda| = 0.6 < 1$.

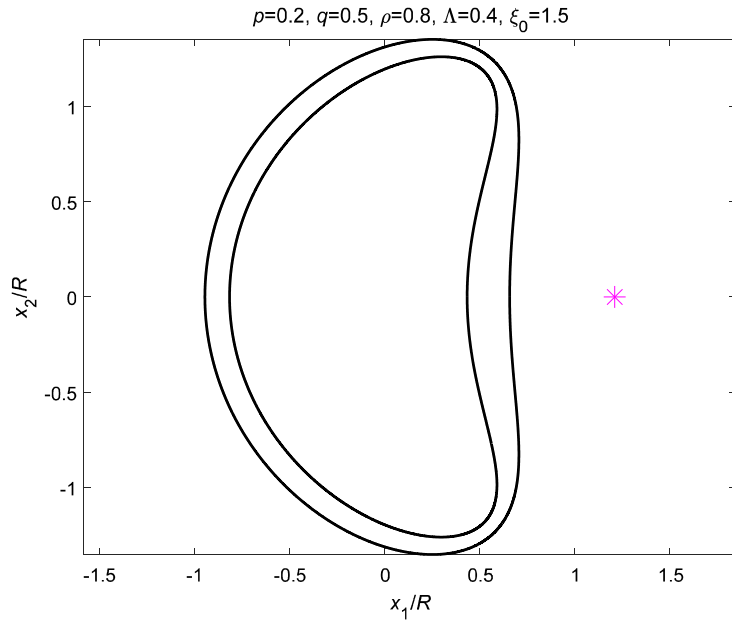


Fig. 3. The shape of the coated inhomogeneity and the location of the screw dislocation by choosing the parameters in Eq. (18). The star is the location of the screw dislocation.

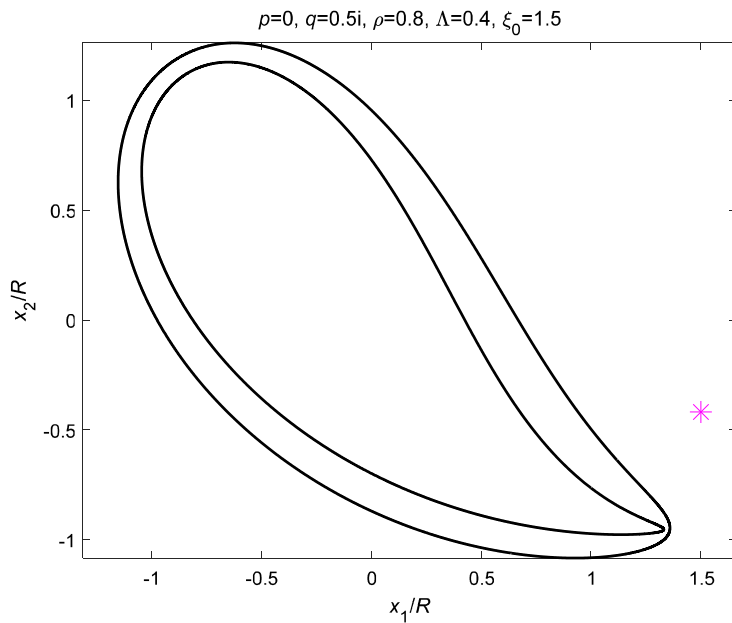


Fig. 4. The shape of the coated inhomogeneity and the location of the screw dislocation by choosing the parameters in Eq. (19). The star is the location of the screw dislocation.

In the final example, the shape of the coated inhomogeneity and the location of the screw dislocation are shown in Fig. 9 for the following parameters

$$p = 0, \quad q = -0.5, \quad \rho = 0.5, \quad \Lambda = -1.2, \quad \xi_0 = 2 \tag{24}$$

In this example, we have $\Lambda < -1$. The series in Eq. (13) again remains convergent since the fact that $\rho|\Lambda| = 0.6 < 1$.

It is clear that, by adjusting the values of the five parameters in the mapping function (13), it is possible to generate many configurations of the three-phase composite admitting our design criterion of an internal uniform stress distribution.

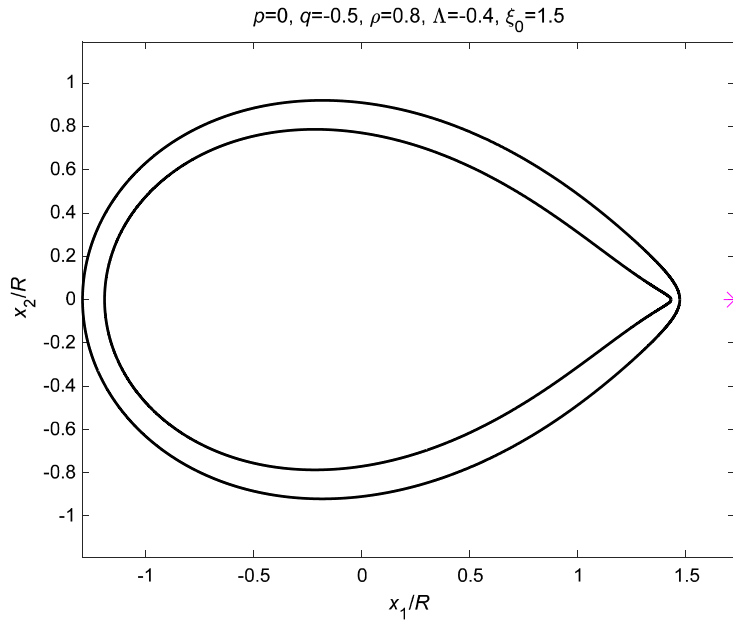


Fig. 5. The shape of the coated inhomogeneity and the location of the screw dislocation by choosing the parameters in Eq. (20). The star is the location of the screw dislocation.

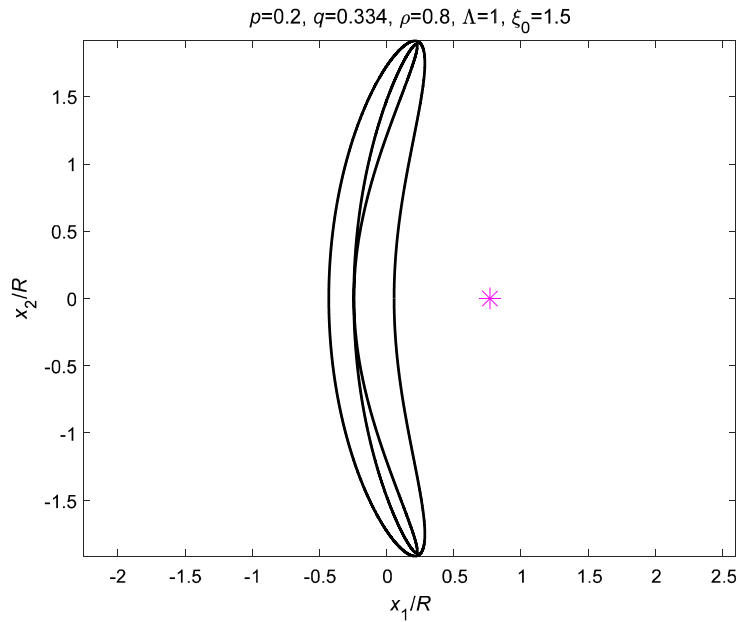


Fig. 6. The shape of the coated inhomogeneity and the location of the screw dislocation by choosing the parameters in Eq. (21). The star is the location of the screw dislocation.

5. Conclusions

We have shown that the internal stress distribution inside a coated non-elliptical inhomogeneity interacting with a screw dislocation under uniform remote stresses can still be maintained uniform when the corresponding composite is subjected to anti-plane shear. The conformal mapping function characterizing the shape of the coated inhomogeneity and the location of the screw dislocation is given explicitly by Eq. (13), which contains five non-trivial parameters, p, q, ρ, Λ , and ξ_0 . The main novelty in our analysis lies in the introduction of the infinite series in the mapping function (13) with a goal to completely removing the logarithmic singularity at the points $\xi = \rho^{-j}\xi_0, j = 1, 2, \dots, +\infty$ in $f_3(\xi)$. Numerical results are presented to validate the feasibility and effectiveness of the solution technique. We mention that our method can be easily

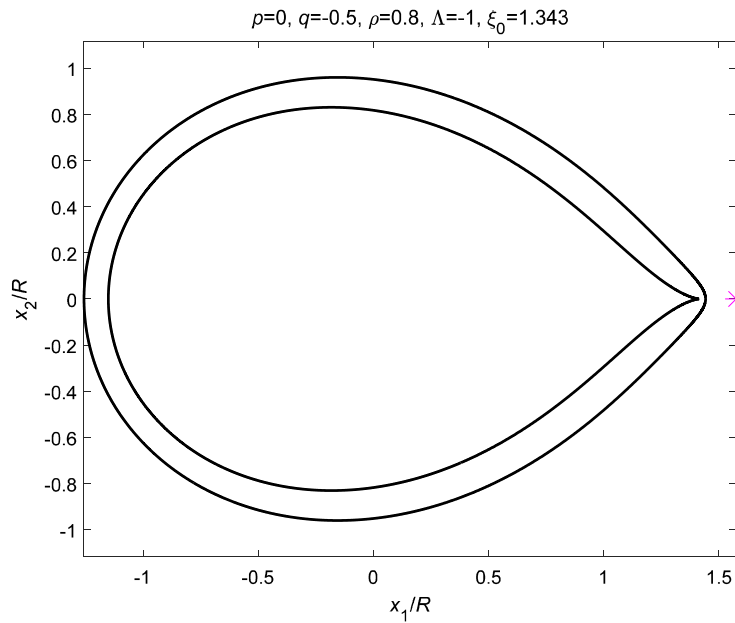


Fig. 7. The shape of the coated inhomogeneity and the location of the screw dislocation by choosing the parameters in Eq. (22). The star is the location of the screw dislocation.

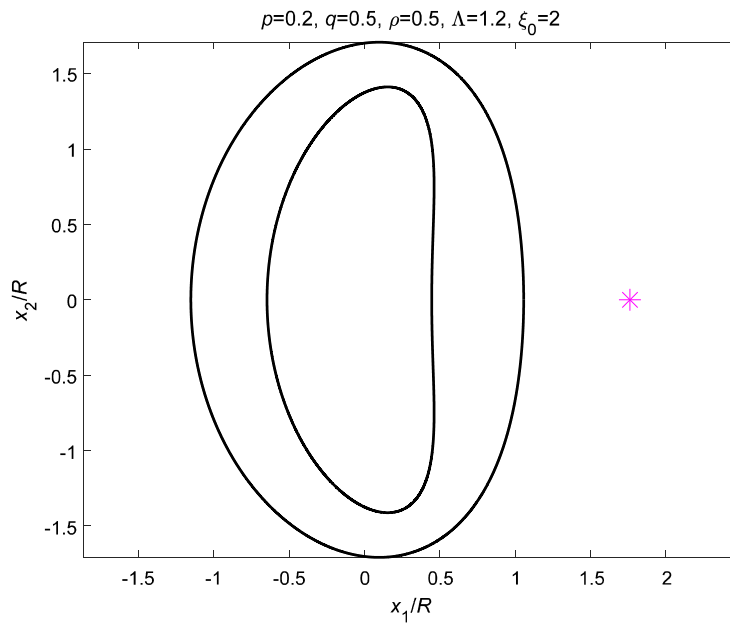


Fig. 8. The shape of the coated inhomogeneity and the location of the screw dislocation by choosing the parameters in Eq. (23). The star is the location of the screw dislocation.

extended to study the uniformity of stresses inside a coated non-elliptical inhomogeneity interacting with an arbitrary number of screw dislocations located in the matrix. In closing, we would like to make two additional comments. Firstly, despite extensive efforts, an extension of our present method to the case of an edge dislocation has not been successful: at this stage we believe such an extension is not possible. Secondly, our method can be applied to the case when the screw dislocation with Burgers vector b is located at $z = z_0$ inside the coating. In this case, the three analytic functions $f_1(z)$, $f_2(\xi)$ and $f_3(\xi)$ are also given by Eqs. (6)–(8). The mapping function is eventually derived as

$$z = \omega(\xi) = R \left(\xi + \frac{p}{\xi} + q \sum_{j=0}^{+\infty} \Lambda^j \ln \frac{\xi - \rho^j \bar{\xi}_0^{-1}}{\xi} + qK \sum_{j=1}^{+\infty} \Lambda^j \ln \frac{\xi - \rho^j \xi_0}{\xi} \right), \quad 1 < |\xi_0| < \rho^{-\frac{1}{2}}, |\xi| \geq 1 \tag{25}$$

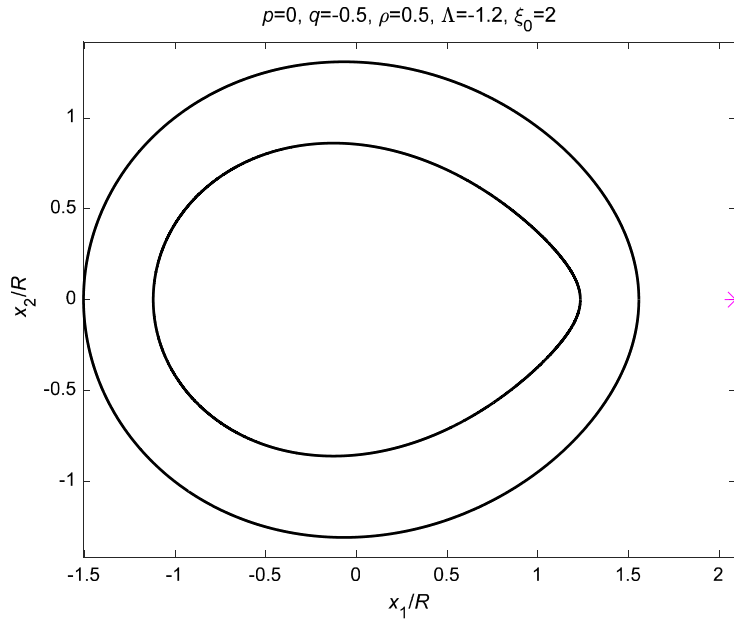


Fig. 9. The shape of the coated inhomogeneity and the location of the screw dislocation by choosing the parameters in Eq. (24). The star is the location of the screw dislocation.

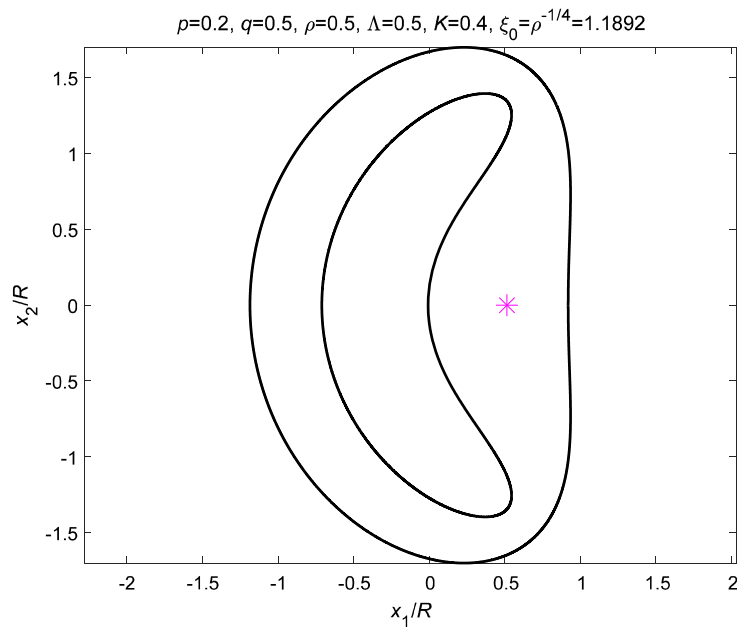


Fig. 10. The shape of the coated inhomogeneity and the location of the screw dislocation with $p = 0.2, q = \rho = \Lambda = 0.5, K = 0.4, \xi_0 = \rho^{-1/4} = 1.1892$ in Eq. (25). The star is the location of the screw dislocation located in the coating.

where Λ has been defined in Eq. (11), $z_0 = \omega(\xi_0)$ and

$$q = \frac{b}{\pi k R (\Gamma_1 - 1)}, \quad K = \frac{\Gamma_1 - 1}{\Gamma_1 + 1} \tag{26}$$

with k being determined by Eq. (15). Both series in Eq. (25) are convergent when $\rho|\Lambda| < 1$. An example of the conformal mapping function in Eq. (25) is illustrated in Fig. 10. In this example, the coating is softer than both the inhomogeneity and the matrix.

Acknowledgements

We are grateful to two reviewers for their valuable comments and suggestions. This work is supported by the National Natural Science Foundation of China (Grant No. 11272121) and through a Discovery Grant from the Natural Sciences and Engineering Research Council of Canada (Grant No.: RGPIN-2017-03716115112).

References

- [1] Y. Mikata, M. Taya, Stress field in and around a coated short fiber in infinite matrix subjected to uniaxial and biaxial loading, *ASME J. Appl. Mech.* 52 (1985) 19–24.
- [2] Y.P. Qiu, G.J. Weng, Elastic moduli of thickly coated particle and fiber-reinforced composites, *ASME J. Appl. Mech.* 58 (1991) 388–398.
- [3] C.Q. Ru, Three-phase elliptical inclusions with internal uniform hydrostatic stresses, *J. Mech. Phys. Solids* 47 (1999) 259–273.
- [4] R. Hashemi, G.J. Weng, M.H. Kargarnovin, H.M. Shodja, Piezoelectric composites with periodic multi-coated inhomogeneities, *Int. J. Solids Struct.* 47 (2010) 2893–2904.
- [5] Y. Benveniste, Exact results for the local fields and the effective moduli of fibrous composites with thickly coated fibers, *J. Mech. Phys. Solids* 71 (2014) 219–238.
- [6] C.Q. Ru, P. Schiavone, A circular inclusion with circumferentially inhomogeneous interface in anti-plane shear, *Proc. R. Soc. Lond. A* 453 (1997) 2551–2572.
- [7] C.Q. Ru, P. Schiavone, A. Mioduchowski, Uniformity of stresses within a three-phase elliptic inclusion in anti-plane shear, *J. Elast.* 52 (1999) 121–128.
- [8] X. Wang, X.L. Gao, On the uniform stress state inside an inclusion of arbitrary shape in a three-phase composite, *Z. Angew. Math. Phys.* 62 (2011) 1101–1116.
- [9] Z.M. Xiao, B.J. Chen, A screw dislocation interacting with a coated fiber, *Mech. Mater.* 32 (2000) 485–494.
- [10] X. Wang, P. Schiavone, Two inhomogeneities of irregular shape with internal uniform stress fields interacting with a screw dislocation, *C. R. Mecanique* 344 (2016) 532–538.
- [11] X. Wang, L. Chen, P. Schiavone, Uniform stress field inside an anisotropic non-elliptical inhomogeneity interacting with a screw dislocation, *Eur. J. Mech. A, Solids* 70 (2018) 1–7.
- [12] T.C.T. Ting, *Anisotropic Elasticity – Theory and Applications*, Oxford University Press, New York, 1996.